9-1-2000

Nanoindentation and Strain Characteristics of Nanostructured Boride/Nitride Films

Niklas Hellgren
Messiah University, nhellgren@messiah.edu

R A. Andrievskii

G V. Kalinnikov

P Sandstrom

D V. Shtanskii

Nanoindentation and Strain Characteristics of Nanostructured Boride/Nitride Films

R. A. Andrievskiĭ, G. V. Kalinnikov, N. Hellgren, P. Sandstrom, and D. V. Shtanskiĭ

Abstract—The hardness, elastic modulus, and elastic recovery of nanostructured boride/nitride films 1–2 μm thick have been investigated by the nanoindentation technique under the maximum loads over a wide range (from 5 to 100 mN). It is demonstrated that only the hardness parameters remain constant at small loads (5– 30 mN). The data obtained are discussed and compared with the parameters determined by other methods.

The basic ideas of investigating strain characteris-tics upon continuous indentation of an indenter were formulated in the mid-1970s (see, for example, [1–5]). This method has been extensively used in studies of films and surface layers, specifically upon nanoindenta-tion under small loads (see, for example, [6–9]). A great body of data on the hardness H and the elastic modulus E was obtained by the indentation technique. In partic-ular, valuable information on films based on interstitial phases (transition metal carbides, nitrides, and borides) was generalized in the review [10]. Interesting tech-niques of examining the microindentation kinetics were proposed by Golovin and Tyurin [11]. However, the observed dependences of H and E on the indenta-tion load P have yet to be unambiguously interpreted, and the reliability of the strain parameters is not univer-sally obvious and is not necessarily discussed. The sole exception is the work of Menchik *et al.* [9], who attempted to unify the techniques of determining E in nanoindentation experiments with ball diamond indent-ers. From general considerations and in relation to the study of size effects in nanostructured materials (spe-cifically in films) [12], it is important to reveal the degree of absolute reliability of the data obtained from nanoindentation measurements.

As a continuation of our earlier work concerned with the determination of the hardness and elastic prop-erties of Ti(B,N) films by conventional methods [13], it was of interest to investigate the same films by the nanoindentation method. The conditions of magnetron sputtering and the characteristics of the $Ti(B_{0.73}N_{0.2}O_{0.05}C_{0.02})_{1.56}$ film (**I**) with a hexagonal structure of the AlB_2 type and the $Ti(N_{0.49}B_{0.34}O_{0.12}C_{0.05})_{1.49}$ film (**II**) with a cubic structure of the NaCl type were given in [13]. Single-crystal silicon wafers were used as substrates. The film thick-nesses were $\delta_I = 1.7–1.8$ μm and $\delta_{II} = 1.2–1.3$ μm.

The structural features were examined by the high-resolution transmission electron microscopy (JEM-3010). The crystallite sizes (L) were estimated on the basis of dark-field images as $L_I = 4–8$ nm for film **I** and $L_{II} = 3–6$ nm for film **II**. Figure 1 shows a micrograph obtained in the direct resolution mode. One can clearly see a characteristic fringe structure and the crystalline character of intercrystalline boundaries. These features were described in detail in our previous work [14].

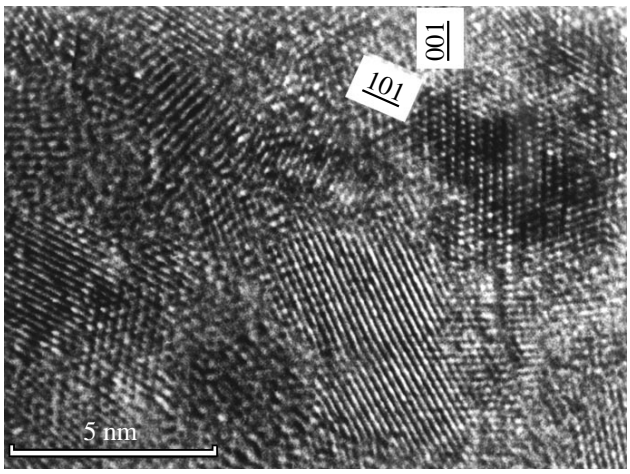

Fig. 1. An image of the structure of film **I** in the direct resolution mode.

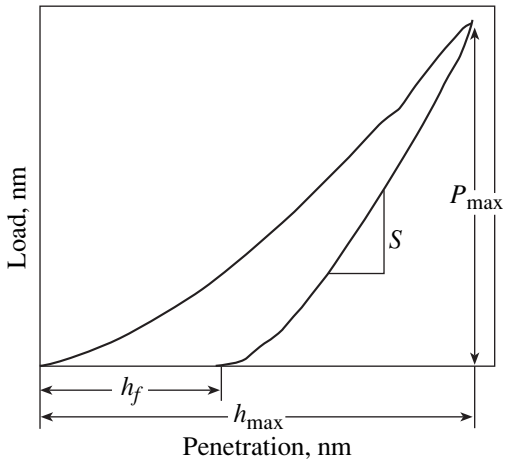

Fig. 2. Schematic representation of the dependences of the load on the penetration of an indenter under loading and unloading.

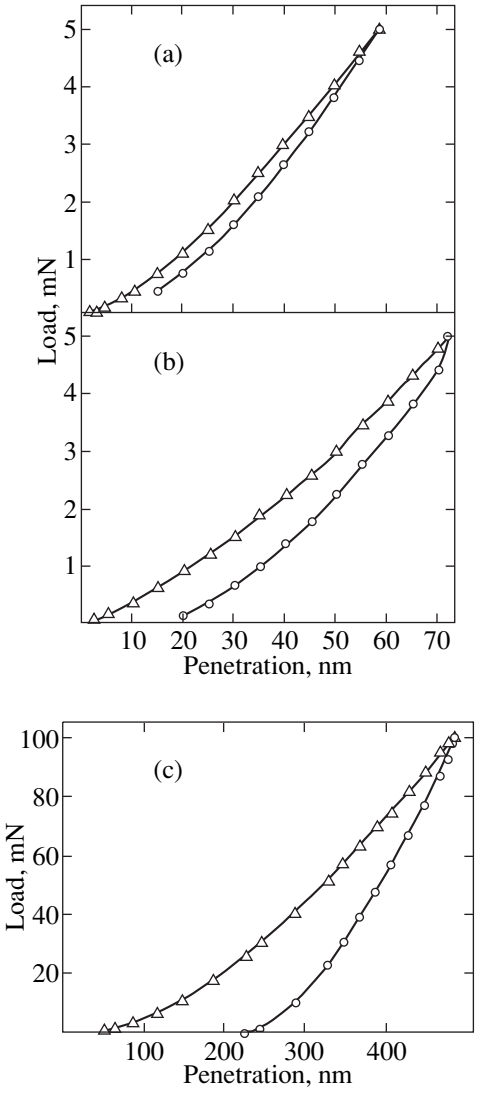

Fig. 3. Experimental loading–unloading curves at (a, b) P_{max} = 5 mN and (c) P_{max} = 100 mN for films (a, c) **I** and (b) **II**.

The nanoindentation measurements were carried out on a Nano Indentor TM II instrument [15] with the use of Berkovich trihedral diamond indenters. The maximum loads P_{max} were equal to 5, 10, 30, and 100 mN. As before (see, for example, [16]), the loading–unloading procedure consisted in loading up to P_{max}, unloading down to $0.1P_{max}$, holding for 50 s, repeated loading to P_{max}, holding for 200 s, and final unloading. At least ten indentations were made for each P_{max} load.

Figure 2 illustrates the loading–unloading scheme and the estimation with the use of the measured parameters. According to the known technique [7], these parameters were used to evaluate $H = P_{max}/A$, $S = dP/dh$, the elastic modulus of the "film + indenter" system $E^* = S/2(\pi/A)^{0.5}$, and the so-called elastic recovery $R = (h_{max} - h_f)/h_{max}$, where A is the indenter projection area determined from the maximum depth of indenter penetration h_{max}. In turn, the elastic modulus of the film E_{film} was calculated from the relationship $1/E^* = (1 - \nu_{ind^2})/E_{ind} + (1 - \nu_{film^2})/E_{film}$, where ν_{ind} and ν_{film} are the Poisson ratios of the indenter and the film ($\nu_{film} \sim 0.2$), respectively; and E_{ind} is the elastic modulus of the indenter (for diamond, E = 1141 GPa and ν = 0.07 [7]).

The experimental loading–unloading curves for the studied films are depicted in Fig. 3. The dependences of the strain characteristics on P are displayed in Fig. 4. As follows from the results obtained, only the hardness H is independent of P at small loads (P = 5–30 mN). The R and E quantities in the studied P range increase with a decrease in the load. Note that brittle films **I** and **II** are almost identical in the elastic recovery, i.e., the very conventional parameter of brittleness (the perfect plasticity and the perfect elastic recovery correspond to R = 0 and 1, respectively), whereas the hardnesses H and the elastic moduli E of the films differ considerably.

In this respect, it is of interest to compare the H and E quantities determined from the nanoindentation measurements with the experimental data obtained by conventional methods. According to [13], $H_I \sim 49$ and E_I = 460 ± 50 GPa for film **I** and $H_{II} \sim 49$ and E_{II} = 480 ± 100 GPa for film **II**. The data on the hardness were obtained with a PMT-3 microhardness tester at a load of 0.3 N and were processed according to the procedure described in [17], which made it possible to eliminate the effect of a softer substrate and differences in film thicknesses on the results of measurements. The Young moduli were determined by the contactless technique of measuring the elastic properties. A comparison of these data with the results demonstrated in Fig. 4 led to the conclusion that different techniques of determining H and E furnish the comparable results for film **I**, whereas the nanoindentation measurements for film **II** give the smaller parameters.

However, this inference requires certain comments. It should be kept in mind that the hardness characteristics obtained in traditional measurements can be larger

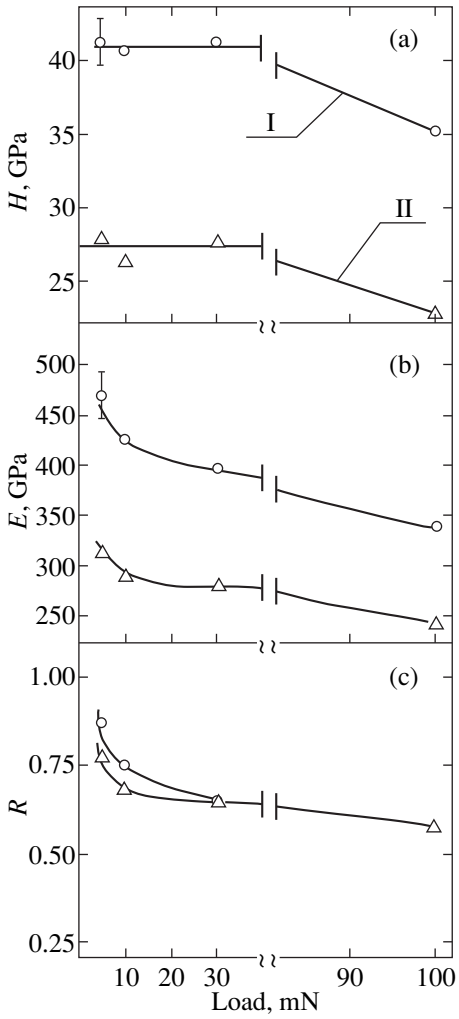

Fig. 4. Effect of the maximum load on (a) hardness, (b) elastic modulus, and (c) elastic recovery.

than those determined by the nanoindentation technique due to the known relaxation effect (the so-called recovered and unrecovered hardnesses). Moreover, it is worth noting that the thicknesses of the studied samples differ, and, hence, the relative depths of indenter penetration h/δ are also different. For example, this ratio at $P = 5$ mN is equal to 0.034 for film **I** and 0.057 for film **II**. At larger loads, this difference becomes all the more evident, and the effect of the substrate should be taken into account. In the general case, the scale effect, i.e., the effect of the indentation load on the strain characteristics, can be due to the scaling violation [18] and the inhomogeneity of the surface layers in the studied objects. As follows from recent publications (see, for example, [19–21]), the surface topography also plays an important part at very small loads (~10 mN and less). The investigation of the Ti(B,N) film surface by the atomic-force microscopy [20] revealed that the relief of films **II** is more developed than that of films **I**, which can be partly responsible for a decrease in the estimates of H and E. Finally, the elastic modulus E evaluated from the nanoindentation data characterizes the strained state under conditions of nonuniform bulk compression. All these factors can affect the measured parameters, but this effect is difficult, if not impossible, to consider them quantitatively

It should be noted that, unlike the results shown in Fig. 4, our earlier nanoindentation experiments [22] made on films **I** with the use of the first nanoindenter model [6] demonstrated a drastic increase in the hardness with a decrease in the load P_{max} from 50 to 10 mN. On the other hand, the errors in measurements of the parameters, specifically of the hardness, sharply increased at small loads (less than 10–20 mN) [20, 23]. On this basis, it is clear that the reliability of strain parameters obtained from the nanoindentation data is rather conventional, and the contribution of possible effects should be considered in detail in each particular case.

ACKNOWLEDGMENTS

We would like to thank Prof. J.-E. Sundgren and Prof. L. Hultman of the Linköping University (Sweden) for their kind attention to the present study.

This work was supported by the International Association of Assistance for the promotion of cooperation with scientists from the New Independent States of the former Soviet Union (project INTAS no. 96-2232), the Program “Integration” (project no. 855), and the Program of the cooperation of the Russian Academy of Sciences and the Royal Swedish Academy of Sciences.

Translated by O. Borovik-Romanova

References

1. A. P. Ternovskiĭ, V. P. Alekhin, M. Kh. Shorshorov, *et al.*, Zavod. Lab. **39**, 1242 (1973).
2. S. I. Bulychev, V. P. Alekhin, M. Kh. Shorshorov, *et al.*, Zavod. Lab. **41**, 1137 (1975).
3. S. I. Bulychev, V. P. Alekhin, M. Kh. Shorshorov, and A. P. Ternovskiĭ, Probl. Prochn., No. 9, 79 (1976).
4. Yu. S. Boyarskaya, D. Z. Grabko, and M. S. Kats, *Phys-ics of Microindentation Processes* (Shtiintsa, Kishinev, 1986).
5. S. I. Bulychev and V. P. Alekhin, *Material Testing by Continuous Indentation of an Indenter* (Mashinostroe-nie, Moscow, 1990).
6. M. F. Doerner and W. D. Nix, J. Mater. Res. **1**, 601 (1986).
7. W. C. Oliver and G. M. Pharr, J. Mater. Res. **7**, 1564 (1992).
8. E. Soderlund and D. J. Rowcliffe, J. Hard Mater. **5**, 149 (1994).
9. J. Menchik, D. Munz, E. Quandt, *et al.*, J. Mater. Res. **12**, 2475 (1997).
10. R. A. Andrievskiĭ, Usp. Khim. **66**, 57 (1997) [Russ. Chem. Rev. **66**, 53 (1997)].
11. Yu. I. Golovin and A. I. Tyurin, Kristallografiya **40**, 884 (1995) [Crystallogr. Rep. **40**, 818 (1995)].
12. R. A. Andrievskiĭ and A. M. Glezer, Fiz. Met. Metallogr. **88**, 50 (1999) [Phys. Met. Metallogr. **88**, 45 (1999)].
13. R. A. Andrievskiĭ, G. V. Kalinnikov, N. P. Kobelev, *et al.*, Fiz. Tverd. Tela (S.-Peterburg) **39**, 1859 (1997) [Phys. Solid State **39**, 1661 (1997)].
14. R. A. Andrievskiĭ, G. V. Kalinnikov, and D. V. Shtanskiĭ, Fiz. Tverd. Tela (S.-Peterburg) **42** (4), 741 (2000) [Phys. Solid State **42**, 760 (2000)].
15. G. M. Pharr, W. C. Oliver, and F. R. Brotzen, J. Mater. Res. **7**, 613 (1992).
16. H. Liungcrantz, C. Engstrom, L. Hultman, *et al.*, J. Vac. Sci. Technol. A **16**, 3104 (1998).
17. B. Jonsson and S. Hogmark, Thin Solid Films **114**, 257 (1984).
18. Yu. V. Mil'man, Probl. Prochn., No. 6, 52 (1990).
19. X. Wang, A. K. Kolitsch, and W. Moller, Appl. Phys. Lett. **71**, 1951 (1997).
20. R. A. Andrievski, in *Surface-Controlled Nanoscale Materials for High-Added-Value Applications*, ed. by K. E. Gonsalves, M.-E. Baraton, R. Singh, H. Hofmann, J. Chen, and J. Akkara (MRS, Warrendale, 1998), Mater. Res. Soc. Symp. Proc. **501**, 149 (1998).
21. R. A. Andrievski, J. Solid State Chem. **133**, 249 (1997).
22. R. A. Andrievskiĭ, S. A. Amanulla, E. J. Brookes, *et al.*, Neorg. Mater. **31**, 1600 (1995) [Inorg. Mater. **31**, 1456 (1995)].
23. G. Shafirstein, M. Gee, S. Osgerby, and S. Saunders, in *Thin Films—Stresses and Mechanical Properties V*, ed. by Sh. Baker, C. Ross, P. Townsend, C. Volkert, and P. Borgesen (MRS, Warrendale, 1995), Mater. Res. Soc. Symp. Proc. **356**, 717 (1995).